

# HYPERPOLARIZED <sup>3</sup>He MRI OF COPD

Lorena Tonarelli, B.Sc. (Hons), M.Sc.

## INTRODUCTION

Over the past decade, there have been major advances in the use of hyperpolarized gas for magnetic resonance imaging (MRI) of respiratory disorders that commonly affect adults and children, such as asthma, chronic obstructive pulmonary disease (COPD), cystic fibrosis, and radiation-induced lung injuries.

This article looks, in particular, at hyperpolarized (HP) helium-3 (<sup>3</sup>He) MRI and its applications to the diagnosis and monitoring of COPD. It first outlines the morphological changes associated with the disease and their importance as diagnostic markers. It then explains the rationale behind the use of hyperpolarized gas in lung MRI, and illustrates the principles of HP <sup>3</sup>He MRI. Based on a review of the research, a description is provided of the four different techniques currently available—static, dynamic, diffusion, and oxygen-sensitive. The limitations of each of these techniques are also discussed, as well as strategies to overcome them.

## OBJECTIVES

After reading this article, the reader will be able to:

1. Explain COPD and how it affects lung morphology
2. Describe how HP <sup>3</sup>He MRI works
3. Discuss its advantages over conventional MRI modalities
4. Illustrate differences and similarities of the various HP <sup>3</sup>He MRI techniques
5. Understand that potential problems are associated with each technique and suggest solutions to mitigate these problems

## COPD

COPD is an umbrella term used to describe various lung disorders, such as emphysema and chronic bronchitis, characterized by incompletely reversible, usually progressive, airflow blockage, and abnormal inflammatory response to inhaled noxious gases and particles.<sup>1,2</sup>

Typical symptoms of COPD include difficulty breathing, cough, and increased sputum production. Chest tightness, fatigue, fluid retention and confusion may also be present.<sup>1,2</sup>

One of the most common respiratory diseases in developed countries, COPD is mainly caused by tobacco use and second-hand smoke. COPD is incurable and life-threatening. It is currently the fourth leading cause of death worldwide, killing more than three million people annually, and is expected to become the third by 2030, according to recent statistics published by the World Health Organization (WHO).<sup>2,3</sup>

### Bronchi, Bronchial Tree, and Lungs

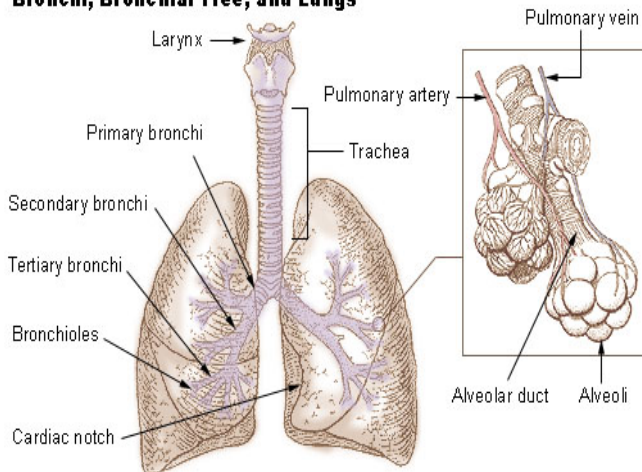


**FIGURE 1.** Anatomy of the lungs and airways. (United States Federal Government diagram)

## MORPHOLOGICAL CHANGES IN COPD

In COPD, the lungs and the airways (Figure 1) undergo a series of morphological changes characteristic of the disease. For example, in emphysema, the air spaces distal to the bronchioles (i.e., the alveoli) become enlarged and the lung tissue (i.e., parenchyma) that

makes up their walls degenerates.<sup>4,5</sup> Changes in the lung arteries, such as vasoconstriction, thickening and hypertrophy, are also typical of COPD disorders, and lead to remodeling of the lung vasculature.<sup>4,5</sup> Furthermore, the airways become progressively narrow and inflamed, with abnormal production of sputum (i.e., a mixture of mucus and saliva).<sup>4-6</sup> These changes (Table 1) are identified well with computed tomography (CT) imaging, which is currently the mainstay diagnostic technique for COPD.<sup>7</sup>

**Table 1. Morphological Changes Characteristic of the Lungs and Airways of Patients with COPD\***

Lung tissue gradually degenerates
Distal airspaces become enlarged
Airways are obstructed by sputum
Lung arteries show thickening and hypertrophy of the walls

\*Data from Ley-Zaporozhan J, Ley S, Kauczor HU. Morphological and functional imaging in COPD with CT and MRI: present and future. *Eur Radiol.* 2008;18:510-21; Saetta M, Baraldo S, Corbino L, et al. CD8+ve cells in the lungs of smokers with chronic obstructive pulmonary disease. *Am J Respir Crit Care Med.* 1999;160:711-7; Szilasi M, Dolinay T, Nemes Z, Starusz J. Pathology of chronic obstructive pulmonary disease. *Pathol Oncol Res.* 2006;12:52-60.

## MRI OF THE LUNGS AND AIRWAYS

Three-dimensional high-resolution computed tomography (3D-HRCT) is the imaging modality of choice for assessment of COPD-related changes like those described in the previous section. However, MRI is becoming increasingly more important for obtaining detailed information about lung function.<sup>5</sup>

Compared to other imaging techniques, MRI is advantageous in that it does not involve the use of ionizing radiation. Moreover, it is highly versatile and allows for the rapid acquisition of accurate data. On the other hand, imaging of the lungs and airways with magnetic resonance is notoriously problematic. First, because this modality exploits the properties of protons for the production of images, and the lungs are mostly made of air; the MRI signal is naturally low. Secondly, the many air-tissue interfaces that characterize the lungs cause magnetic field inhomogeneities (due to the high magnetic susceptibility difference between air and tissue), which also diminishes the strength of the MRI signal. Other problems include poor spatial resolution and motion artifacts caused by cardiac pulsation and respiratory activity.<sup>8-10</sup>

The above imaging issues are common to all lungs and airways. Additional problems exist when COPD is present. This is because patients with the disease suffer from progressive loss of lung tissue and blood volume, which further contribute to diminished MR signal strength.<sup>5</sup>

## HYPERPOLARIZED HELIUM MRI

We have seen so far that conventional magnetic resonance techniques are difficult to use in lung imaging, which limits their clinical utility for respiratory disorders, such as COPD.

However, recent advances in MRI pulse sequences, the development of more sophisticated hardware and software, and the introduction of contrast agents have significantly improved image quality in MRI of the lung parenchyma and function.<sup>8-10</sup> Of particular interest, in this regard, is the use of inhaled hyperpolarized (HP) noble gases, such as helium and xenon. Both can be used in lung MR imaging, although helium is generally preferred, for two main reasons: it provides higher signal-to-noise ratios (SNRs), and, after inhalation, it remains conveniently confined to the airways and air spaces, rather than being absorbed by the surrounding tissues or into the bloodstream.<sup>11,12</sup>

Hyperpolarized helium (HP <sup>3</sup>He) is produced by laser optical pumping (OP), which involves irradiating the gas with a high-powered laser light. The procedure is carried out outside the MRI unit using a special device, and lasts for a period of minutes to hours. Irradiation increases the spin polarization of the gas to values several orders of magnitude larger than those achievable with standard MRI magnets, which, in turn, translates into a stronger signal. The hyperpolarized gas becomes a source of nuclear magnetic resonance (NMR) signal with improved signal-to-noise ratio, and can be used as an inhaled contrast agent to image lung tissue, air space, and function under static (i.e., during breath hold) and dynamic (i.e., during breathing) conditions.<sup>11,12</sup>

Once hyperpolarized, the helium is usually mixed with helium-1 and is handed to the patient within the scanner, who is instructed to inhale the gas, either from an inhaler or a sealed bag. The gas is inhaled by the patient after full expiration.<sup>11,13,14</sup> Importantly, the polarization of helium is rapidly lost through T1-relaxation if the gas is exposed to oxygen in the air—a phenomenon known as the paramagnetic effect of oxygen. Loss of polarization also occurs as a result of the Brownian motion of the gas in the presence of macroscopic B<sub>0</sub> field gradients, and because of microscopic field variations generated when the gas comes into contact with magnetic impurities in the wall of the storage container. Thus, hyperpolarized helium has to be adequately handled, stored and transported to minimize the loss of polarization. It should be given to the patient swiftly, preferably in less than five seconds, and inhaled promptly.<sup>13</sup>

The acquisition window for a hyperpolarized pulse sequence is also limited. Imaging should start immediately after inhalation. For hyperpolarized <sup>3</sup>He MRI examinations performed during breath-hold, the acquisition time, which depends on section thickness, needs to be adjusted to the patient's ability to hold their breath.<sup>11,13,14</sup>

The enhanced signal from the lung air spaces, generated after inhalation, is detected by radiofrequency (RF) coils, whose characteristics are extremely important to ensure high signal-to-noise ratios. The coils need to be tuned to the Larmor frequency of the gas. At 1.5 Tesla, this is 48.66 MHz. They can be of different shape (e.g., birdcage, surface), but they must cover the field-of-view (FOV) of lungs and airways. This generally corresponds to 30 x 30 x 18 cm<sup>2</sup>. The signal is then measured using high spatial and temporal resolution 3D MRI. Thus, it is possible to study the gas flow into the lung air spaces (i.e., ventilation) and into the airways (i.e., spirometry). The transmit coil should generate the same excitation angle throughout the lungs, for a series of flip angles.<sup>11-13</sup>

The performance and clinical utility of HP <sup>3</sup>He MRI has been evaluated in studies of healthy subjects and patients with respiratory diseases, with low-field (0.1 and 0.54 Tesla), high-field (1.5 Tesla), and ultra-high-field (3.0 Tesla) systems.<sup>15,16</sup> It is important to note that there is no correlation between the polarization of helium and the strength of the static magnetic field B<sub>0</sub> generated by the MRI scanner. Therefore, it is possible to obtain high signal-to-noise ratio images at low, and even very low, field strengths.<sup>17,18</sup> Although the most favorable magnetic field strength for hyperpolarized helium imaging remains to be determined, high-quality images and clinically-useful data are generally obtained with high-field (1.5 Tesla) and ultra-high-field (3.0 Tesla) systems.<sup>16,19</sup>

Of particular significance in this regard are the results of a recent study where hyperpolarized <sup>3</sup>He MR imaging at 1.5 Tesla enabled the detection of ventilation defects due to peripheral airway obstruction in patients who were asymptomatic and whose spirometric test results showed normal lung function.<sup>19</sup>

Hyperpolarized <sup>3</sup>He MRI is mostly performed with a low-flip angle, fast-low angle shot (FLASH) sequence, although other sequences can be used, such as interleaved echo planar, interleaved-spiral, and multi-spin echo.<sup>12,15</sup> With respect to the possibility of artifacts, at 0.54 Tesla, interleaved spiral images have been associated with less blurring from susceptibility-induced magnetic field inhomogeneities than at 1.5 Tesla.<sup>15</sup>

## HP <sup>3</sup>He MRI IN COPD

Hyperpolarized <sup>3</sup>He MRI includes four techniques, each of which allows for the examination of a different aspect of lung function.<sup>11</sup> These techniques are:

- \* Static ventilation hyperpolarized <sup>3</sup>He MRI
- \* Dynamic ventilation hyperpolarized <sup>3</sup>He MRI
- \* Diffusion hyperpolarized <sup>3</sup>He MRI
- \* Oxygen-sensitive hyperpolarized <sup>3</sup>He MRI

All of these techniques are clinically useful in the diagnosis and management of COPD, and are described in

**Table 2. Hyperpolarized <sup>3</sup>He MRI Techniques: Main Characteristics and Applications\***

Technique	Clinical Use	Data Acquisition	Limitations
Static ventilation HP <sup>3</sup> He MRI	Detection of ventilation abnormalities	Gradient-echo sequences (e.g., FLASH, FISP) during breath hold	Volumetric measurements derived from thick-slice gradient-echo images may be difficult, due to signal loss caused by background field gradients
Dynamic ventilation HP <sup>3</sup> He MRI	Detection of ventilation abnormalities during the respiratory cycle	Ultra-fast echo-planar (EPI), gradient-echo, and interleaved spiral sequences; no breath hold required	Diffusion-induced signal loss leading to low spatial resolution, and motion or other artifacts may occur, when using an EPI sequence
Diffusion HP <sup>3</sup> He MRI	Assessment of the lungs' microstructure (i.e., size, morphology, and distribution of distal airways and airspaces)	Gradient-echo-based or stimulated-echo-based pulse sequences during breath hold	Long diffusion times are a potential source of diagnostic error
Oxygen-sensitive HP <sup>3</sup> He MRI	Measurement of regional lung function (i.e., oxygen pressure, concentration, and depletion rate)	Gradient-echo sequences (e.g., FLASH) during either one or two breath holds	Errors in oxygen pressure measurements may occur due to inter-slice gas diffusion from long inter-image delay times, when using a two-dimensional sequence

\*Data from: Baert AL, Knauth M, Sartor K. MRI of the Lung. Berlin Heidelberg, Germany: Springer-Verlag; 2009; Hopkins SR, Levin DL, Emami K, et al. Advances in magnetic resonance imaging of lung physiology. *J Appl Physiol.* 2007;102:1244-54; van Beek EJ, Wild JM, Kauczor HU, Schreiber W, Mugler JP 3rd, de Lange EE. Functional MRI of the lung using hyperpolarized 3-helium gas. *J Magn Reson Imaging.* 2004;20:540-54; Kauczor HU, Hofmann D, Kreitner KF, et al. Normal and abnormal ventilation: visualization at Hyperpolarized He-3 MR Imaging. *Radiology.* 1996;201:564-8.



detail in the next sections. A summary of their main characteristics and applications is provided in Table 2.

## STATIC VENTILATION HP $^3\text{He}$ MRI

Static ventilation imaging—also referred to as spin-density imaging—provides information about the distribution of  $^3\text{He}$  in the distal lung air spaces, from which ventilation abnormalities (i.e., reduced ventilation, or hypoventilation) can be detected. Patients are instructed to inhale hyperpolarized helium and to hold their breath in maximum inspiration for about 20 to 40 seconds. A nose clamp is applied to prevent the patient from breathing through the nose.<sup>14</sup>

Static ventilation imaging uses both 2D and 3D gradient-echo sequences, mainly FLASH sequences. Although 2D acquisitions have been preferred for some time, 3D acquisitions are increasingly being used because of their improved signal-to-noise ratio. In a comparative study, the mean SNR was 1.4 and 1.7 times greater with the 3D method, for lungs and airways, respectively.<sup>20</sup>

An example of the application of 3D gradient-echo sequences for spin density imaging can be found in a study of healthy subjects and patients with lung diseases, including COPD, where high-resolution visualization of ventilation defects was achieved using T1-weighted 3D FLASH. This was performed on a high-field (1.5 Tesla) whole body MRI unit, using the following scanning parameters<sup>14</sup>:

- Repetition time: 11.8 msec
- Echo time: 5 msec
- Matrix size: 144 x 256
- Field-of-view: 350 mm
- Flip angle: less than 5°

As noted earlier, section thickness and corresponding image acquisition time must be carefully determined based on the patient's breath-holding capabilities. For example, in this study, section thickness was 7.0, 8.33, or 10 mm—corresponding to image acquisition times of 42, 32 and 22 seconds, respectively.<sup>14</sup>

After inhalation, air spaces with no ventilation defects are filled with the gas. Thus, because of the high signal-to-noise ratio associated with hyperpolarized helium, they show in FLASH images as bright, hyperintense (i.e., high signal intensity) areas. On the other hand, if airflow obstruction is present, the level of hyperpolarized helium is reduced in affected air-spaces. Therefore, ventilation defects appear as dark, hypointense (i.e., low signal intensity) areas, usually wedge- or focal-shaped. In practical terms, this means that static ventilation images of healthy subjects (i.e., no defects) are characterized by homogeneous high-signal intensity, whereas those of patients with severe

COPD are characterized by marked signal intensity inhomogeneity.<sup>14</sup>

In healthy subjects, static ventilation images may include areas that appear less ventilated than others. This is due to differential distribution of the gas as a result of gravity and patient position, and can be misinterpreted for ventilation defects. The hypoventilated areas are usually visible in the most posterior parts of the lungs, for subjects imaged in the supine position, and in the most anterior parts of the lungs for subjects imaged in the prone position.<sup>21</sup>

Gradient-echo sequences other than FLASH have also been used for static ventilation imaging, including steady state free precession (FISP). It has been demonstrated that, at 1.5 Tesla, FISP allows for a three-fold signal-to-noise ratio increase compared to FLASH, but susceptibility artifacts can occur. These can be corrected by implementing FISP at low-field strength.<sup>22</sup>

Although ventilation defects are easily detectable with spin density images, quantitative assessments of their severity through volumetric analyses remain difficult. For example, it has been demonstrated that volumetric measurements of lung ventilation from thick-slice gradient-echo images are associated with signal loss as a result of background field gradients. This loss can be mistaken for ventilation defects. The problem can be minimized, but not avoided altogether, by applying a multiple acquisition interleaved single gradient echo sequence, whose slice refocus gradients are increased to compensate for the loss of signal.<sup>23</sup>

Measurements of ventilated lung volumes have also been performed in studies by segmenting the lung in a proton MR image and then subtracting the corresponding  $^3\text{He}$  MR image. This subtraction method provides information about lung volumes actually ventilated in each slice. However, it has limited proven clinical efficacy, given that it has been used, so far, only in patients with mild COPD.<sup>24</sup>

## DYNAMIC VENTILATION HP $^3\text{He}$ MRI

The high signal-to-noise ratio and short repetition time of hyperpolarized helium MRI make it possible to perform examinations of lung function during the respiratory cycle. Known as dynamic ventilation HP  $^3\text{He}$  MR imaging, this technique provides the means to follow the movements of the inhaled gas bolus and, in turn, to visualize the distribution of the gas during breathing. Quantitative assessments of the regional distribution of lung ventilation can then be made.<sup>25</sup>

Dynamic ventilation HP  $^3\text{He}$  MRI is, therefore, a valuable tool for identifying airflow abnormalities and assisting with the differentiation of diseased from healthy lungs. Dynamic ventilation images of COPD patients are characterized by nonuniform distribution of the gas throughout the lungs, as a result of airways obstructions, air trapping, and other problems which

hinder the movement of the gas bolus after inhalation. In contrast, images of healthy subjects, with no airway obstructions, show homogeneous distribution of the gas throughout the lungs.<sup>11</sup>

Dynamic ventilation HP  $^3\text{He}$  MRI provides greater spatial resolution and image detail than standard diagnostic imaging methods for COPD, such as radiolabeled aerosol scintigraphy. It also provides high temporal resolution because it uses MR pulse sequences that allow multiple image acquisition in a very short time (i.e., less than one second). These include ultra-fast echo-planar (EPI), gradient-echo, and interleaved spiral sequences.<sup>11</sup>

Notably, one study including patients with severe COPD has demonstrated that imaging of the flow and distribution of hyperpolarized  $^3\text{He}$  in the lungs with echo-planar MR pulse sequences can reveal abnormalities not detected with radiolabeled aerosol scintigraphy.<sup>26</sup> Transaxial MRI was performed on a 1.5 Tesla whole body system, using an EPI sequence with the following parameters<sup>26</sup>:

- Repetition time: 40.5 msec
- Echo time: 12.1 msec
- Echo train length: 32
- Matrix size: 32 x 64
- Field-of-view: 225 x 450 mm
- Pixel size: 7 mm<sup>2</sup>
- Flip angle: 22°
- Section thickness: 10 mm

EPI has advantages, such as the fact that it allows several excitations with a reduced use of the hyperpolarization of helium. This is important, for the latter is non-renewable; some of it is consumed during each acquisition and can only be restored via inhalation of additional hyperpolarized gas.<sup>27</sup> However, EPI also has limitations, such as diffusion-induced loss of the MR signal leading to decreased spatial resolution, and susceptibility to artifacts.<sup>26,27</sup> Using an interleaved EPI (I-EPI) pulse sequence can minimize these problems, although motion artifacts, to which I-EPI is particularly susceptible, remain.<sup>28,29</sup>

A useful application of hyperpolarized  $^3\text{He}$  magnetic resonance is for producing images that show differential contrast enhancement of both the distal airways and the lung periphery. Unlike static ventilation imaging, where the airways are hidden by the lung periphery, dynamic imaging allows for the production of images where the airways are clearly depicted. This has been achieved, for instance, with a fast gradient-echo (GRE) pulse sequence on a 1.5 Tesla unit (General Electric Medical Systems).<sup>30</sup>

Imaging was performed during inhalation of 500 mL

of hyperpolarized  $^3\text{He}$ . Inhalation usually lasts five to eight seconds, and no breath hold is needed. Scanning parameters included<sup>30</sup>:

- Repetition time: 1.2 msec
- Echo time: 4.4 msec
- Matrix size: 160 x 128
- Field-of-view: 460 mm
- Delay after acquisition: 50 msec
- Flip angle: 9° to 25°

Note how the flip-angle values used in the study ranged between two values. This is because manipulating the flip angle made it possible to modify the number of distal airways and amount of lung periphery depicted in the images. Smaller flip angles allow more lung periphery to be visualized. Greater flip angles allow more airways to be visualized. However, the greater the flip angle the more hyperpolarized gas magnetization is destroyed, and this magnetization is nonrenewable. Thus, flip angles greater than a certain value—usually 30 degrees—should be avoided, as they yield too little information.<sup>30</sup>

Dynamic ventilation imaging can be performed just after a breath hold examination. This allows the rate of gas clearance to be measured and identifies airflow abnormalities in patients with obstructive lung disease.<sup>31</sup> The procedure has the advantage in that only one dose of helium—which is costly and available only in limited quantities—can be used for two ventilation imaging exams (static and dynamic).

## DIFFUSION HP $^3\text{He}$ MRI

An important property of hyperpolarized  $^3\text{He}$  is its very high diffusion coefficient. In the air, this is 0.88 cm<sup>2</sup>/second. However, after inhalation, the gas diffusion (i.e., Brownian motion) becomes restricted by the walls of the lung's air spaces and by the small size of the airways. For this reason, the rate of helium diffusion is expressed as *apparent diffusion coefficient* (ADC) value.<sup>13</sup>

In the presence of a magnetic field, diffusion attenuates the MRI signal. Thus, sequences can be used to measure the ADC of inhaled hyperpolarized  $^3\text{He}$ . These measurements are particularly useful in the evaluation of the lung's microstructure.<sup>13</sup>

Diffusion measurements are generally performed with the pulsed-gradient spin-echo (PGSE) method using two pulsed gradients separated by a diffusion time ( $\Delta$ ), with or without a 180-degree refocusing pulse. ADC values of 0.1 to 0.2 cm<sup>2</sup>/second are typical of the lungs of healthy subjects, whereas higher values (up to 0.5 cm<sup>2</sup>/second) are characteristic of the lungs of emphysema patients. Such an increase in ADC reflects the fact that the gas movement is less restricted, as some

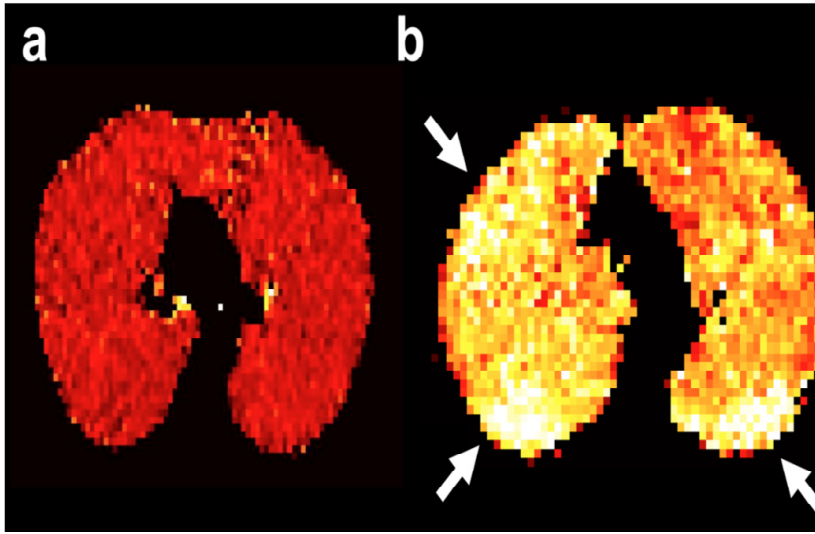


**FIGURE 2.** Apparent diffusion coefficient (ADC) maps of the lung from hyperpolarized helium-3 MRI. (a) Axial helium-3 ADC map from a healthy subject. The ADC values are relatively low and uniform, reflecting the relatively small airspaces, with a narrow distribution of sizes, in the parenchyma of the healthy lung. (b) Axial helium-3 ADC map from a subject with emphysema (COPD). The ADC values are elevated compared to those for the healthy subject, and show regions of focal increases (e.g., arrows), reflecting the enlargement of airspaces which accompanies lung-tissue destruction in emphysema. (c) Axial CT image from the emphysema subject in (b), at approximately the same level. Note the strong correlation between regions of lung-tissue loss seen in the CT image (areas of hypodensity) and focal increases in values in the ADC map (arrows). (Images and caption courtesy of Professor John Mugler III, of the Center for In-vivo Hyperpolarized Gas MR Imaging, University of Virginia)

of the walls of the lung's air spaces have been destroyed as a result of the disease. In other words, in emphysematous patients, lung tissue progressively degenerates, leading to enlarged air spaces. Consequently,  $^3\text{He}$  moves more freely (i.e., higher diffusion), which is reflected in higher than normal ADC values. The higher the ADC, the more severe the emphysema (Figure 2).<sup>13</sup>

It is important to choose the diffusion time  $\Delta$  (delta) carefully, as this affects the reliability of the results. Delta is the amount of time  $^3\text{He}$  is allowed to diffuse inside the lungs in order to measure the signal attenuation.<sup>32</sup> Usually, ADC measurements are performed using diffusion times of a few milliseconds, during which the gas can travel a few hundred microns. These are referred to as *short-time scale* measurements. Longer  $\Delta$  values mean the gas can travel longer distances. This increases the chance of it coming into contact with undamaged walls that restrict its movement, resulting in ADC values lower than what they actually are.<sup>13,32</sup>

In diffusion hyperpolarized  $^3\text{He}$  MR, imaging is performed during one single breath hold, as with static ventilation. At least two images are acquired at each section position, providing diffusion data from which ADC maps can be calculated. In ADC maps, the higher the diffusion of  $^3\text{He}$ , the higher the intensity of the signal, and the brighter the area on the map. Compared to ADC maps of healthy subjects, where the diffusion coefficient, and

therefore lung ventilation, is more or less uniform across the lungs, ADC maps of patients with emphysema show regional variations of diffusion coefficients and, as mentioned earlier, larger diffusion values.<sup>32,33</sup>

ADC maps are usually accompanied by a histogram displaying ADC values (in  $\text{cm}^2/\text{second}$ ) on the x-axis and pixel count on the y-axis. Studies have shown that it is possible to use ADC data from maps and histograms to obtain detailed information about the actual size, morphology, and distribution of distal airways and air spaces. This represents a major advantage compared with ventilation imaging, where the acquired data only reflect the presence of the gas, without accounting for the changes that occur in airways and airspaces, like enlargement and tissue degeneration, as a result of the disease.<sup>34</sup>

As discussed earlier, to avoid a potential source of diagnostic error, most ADC measurements are acquired using short diffusion times of a few milliseconds. However, given the small distance  $^3\text{He}$  can travel during this short time, such measurements only provide information about small lung regions.<sup>32</sup> Research shows that, in contrast, ADC measurements performed with long diffusion times (i.e., tens of milliseconds to several seconds) allow the investigation of larger areas and, in turn, provides information about the structures that connect the air spaces. Thus, long-time scale ADC measurements could, in fact, be more sensitive than short-time scale measurements for detecting disease-



related changes in the lung microstructure.<sup>32</sup>

This has been confirmed by work conducted on healthy subjects and patients with respiratory pathologies, such as COPD and bronchopulmonary dysplasia. Diffusion times ranged from 2 milliseconds to 6.5 seconds. Imaging was performed on a 1.5 Tesla system using a gradient-echo-based pulse sequence for short-time scale ADC measurements, and a stimulated-echo-based pulse sequence for long-time scale ADC measurements. As expected, the apparent diffusion coefficient of hyperpolarized  $^3\text{He}$  decreased as the diffusion time increased. However, lung regions damaged by disease, which we have seen earlier are characterized by higher apparent diffusion coefficient compared with healthy tissue, and appear as bright hyperintense areas on ADC maps, were significantly more visible in maps acquired with long diffusion times than in maps acquired with short diffusion times.<sup>32</sup>

### OXYGEN-SENSITIVE HP $^3\text{He}$ MRI

The loss of  $^3\text{He}$  hyperpolarization through T1 relaxation that normally happens after inhalation is markedly accelerated in the presence of oxygen. Furthermore, it occurs at a rate that is proportional to the concentration of oxygen. This has prompted researchers to explore the idea that this phenomenon could be exploited to measure regional lung function, based on data relative to the distribution of oxygen. Animal and human studies have confirmed the hypothesis, and shown that hyperpolarized  $^3\text{He}$  MRI is a clinically useful, non-invasive, method for depicting, not only regional lung ventilation, but also regional lung oxygen partial pressure ( $p\text{O}_2$ ) and oxygen concentration ( $[\text{O}_2]$ ).<sup>35-37</sup>

Early applications of oxygen-sensitive imaging made it possible to measure regional lung oxygen partial pressure with great accuracy. However, data acquisition was performed during two breath holds, which is susceptible to poor breath hold reproducibility and consequent misregistration artifacts, due to the difficulty of replicating the first breathing maneuver.<sup>36</sup> Therefore, the double-acquisition approach was later modified to require only one breath hold, using a 2D FLASH gradient-echo sequence on a 1.5 Tesla system. The single-acquisition sequence reduces the occurrence of artifacts and enables high-temporal resolution measurements of regional  $p\text{O}_2$  and  $[\text{O}_2]$ , from which the oxygen depletion rate (i.e., the rate at which oxygen moves from the air spaces into the bloodstream) can be derived using the following equation<sup>35;37-39</sup>:

$$S(t) = S(0) - \Gamma \cdot P_A \text{O}_2 \cdot t + 1/2R \cdot t^2 \quad (1)$$

Where

- $S(t)$  is the MRI signal intensity at time  $t$ ;
- $S(0)$  is the signal intensity at baseline;
- $P_A \text{O}_2$  is the oxygen pressure in the distal air spaces;

- $R$  is the oxygen depletion rate; and
- $\Gamma$  (tau) is the proportionality constant between oxygen pressure and the relaxation rate of  $^3\text{He}$ .

Since oxygen depletion depends on lung perfusion (i.e., blood flow), oxygen pressure measurements also allows for the calculation of the regional ventilation-to-perfusion ratio ( $V_A/Q$ )—a key parameter for depicting lung function.<sup>38,40</sup>

It is important to note, however, that the 2D sequence used in the studies mentioned above requires inter-image delay times of up to several seconds, which may result in  $p\text{O}_2$  measurement errors due to inter-slice gas diffusion. This problem can be overcome by measuring  $p\text{O}_2$  with a 3D gradient-echo sequence.<sup>41</sup>

### CONCLUSIONS

COPD is an incurable disorder characterized by difficult breathing due to airflow blockage and inflammation. COPD lungs show morphological changes, such as larger airspaces and tissue degeneration, which can be identified with CT.

Although CT is the current standard for diagnosing and monitoring COPD, MRI is becoming increasingly useful, allowing for rapid and accurate data acquisition without the use of ionizing radiation. However, insufficient signal strength due to the lung's low proton density and magnetic field inhomogeneities limit the use of conventional MRI techniques. Therefore, hyperpolarized helium produced via optical pumping is used as an inhaled contrast agent to increase the strength of the signal, thereby improving image quality and clinical utility.

There are four different hyperpolarized  $^3\text{He}$  MRI techniques, each of which has a different use:

- \* *Static ventilation hyperpolarized  $^3\text{He}$  MRI* shows how the inhaled gas is distributed throughout the lungs, allowing for the visualization of ventilation defects. Image data acquisition occurs during breath hold with gradient-echo sequences, such as FLASH and FISP. Both two- and three-dimensional sequences can be used, but the latter result in improved signal-to-noise ratio. Volumetric measurements can be difficult, due to signal loss caused by background field gradients. However, this problem can be mitigated with the application of a multiple acquisition interleaved single gradient echo sequence.
- \* *Dynamic ventilation hyperpolarized  $^3\text{He}$  MRI* detects ventilation defects by visualizing the gas distribution throughout the lungs during the respiratory cycle, so no breath hold is needed. Commonly used sequences include ultra-fast echo-planar (EPI), gradient-echo, and interleaved spiral. Artifacts as well as low spatial resolution due to diffusion-induced signal loss may occur with EPI sequences. Applying an interleaved EPI pulse sequence can overcome some of these problems, but motion artifacts usually remain.

- \* *Diffusion hyperpolarized <sup>3</sup>He MRI* allows the assessment of the lungs' microstructure (i.e., size, morphology, and distribution of distal airways and airspaces) through measurements of the apparent diffusion coefficient of helium. Compared to healthy lungs, COPD lungs have higher ADC due to the enlargement of the distal airways characteristic of the disease. Measurement errors may occur, but can be prevented by using diffusion times of a few milliseconds. On the other hand, ADC measurements performed with longer diffusion times have proven more sensitive for detecting COPD-related changes in the lungs' microstructure. Data acquisition is performed during breath hold, using a gradient-echo-based pulse sequence for short diffusion time measurements, or a stimulated-echo-based pulse sequence for long diffusion time measurements.
- \* *Oxygen-sensitive hyperpolarized <sup>3</sup>He MRI* measures regional lung function (i.e., oxygen pressure, concentration, and depletion rate) by exploiting the paramagnetic effect of oxygen on hyperpolarized helium. Like static ventilation imaging, this technique uses gradient-echo sequences, such as FLASH. Image data acquisitions are performed during either one or two breath holds, although using two breath holds may cause misregistration artifacts. Furthermore, 2D sequences are associated with oxygen pressure measurement errors due to inter-slice gas diffusion from long image delay times. These can be prevented by employing 3D sequences.

## REFERENCES

- World Health Organization (WHO). *Chronic Obstructive Pulmonary Disease (COPD)*. Available at: <http://www.who.int/respiratory/copd/en/index.html>. Accessed April 5, 2011.
- World Health Organization (WHO). *Chronic Obstructive Pulmonary Disease: Factsheet*. Available at: <http://www.who.int/mediacentre/factsheets/fs315/en/index.html>. Accessed April 5, 2011.
- World Health Organization (WHO). *World Health Statistic 2008*. World Health Organization 2008. Available at: <http://www.who.int/whosis/whostat/2008/en/index.html>. Accessed April 5, 2011.
- Szilasi M, Dolinay T, Nemes Z, Strausz J. Pathology of chronic obstructive pulmonary disease. *Pathol Oncol Res*. 2006;12:52-60.
- Ley-Zaporozhan J, Ley S, Kauczor HU. Morphological and functional imaging in COPD with CT and MRI: present and future. *Eur Radiol*. 2008;18:510-21
- Saetta M, Baraldo S, Corbino L, et al. CD8+ve cells in the lungs of smokers with chronic obstructive pulmonary disease. *Am J Respir Crit Care Med*. 1999;160:711-7.
- Sverzellati N, Molinari F, Pirroni T, Bonomo L, Spagnolo P, Zompatori M. New insights on COPD imaging via CT and MRI. *Int J Chron Obstruc Pulmon Dis*. 2007;2:301-12.
- Kauczor HU, Kreitner KF. MRI of the pulmonary parenchyma [German]. *Eur Radiol*. 1999;9:1755-64.
- Leutner C, Schild H. MRI of the lung parenchyma. *Rofö*. 2001;173:168-75.
- Hatabu H, Chen Q, Stock KW, Gefter WB, Itoh H. Fast magnetic resonance imaging of the lung. *Eur J Radiol*. 1999;29:114-32.
- van Beek EJ, Wild JM, Kauczor HU, Schreiber W, Mugler JP 3rd, de Lange EE. Functional MRI of the lung using hyperpolarized 3-helium gas. *J Magn Reson Imaging*. 2004;20:540-54.
- Leduc M, Nacher PJ, Sinatra A, et al. Hyperpolarized 3HE gas MRI. Available at: [www.lkb.ens.fr/recherche/flquant/HPG.html](http://www.lkb.ens.fr/recherche/flquant/HPG.html). Accessed April 8, 2011.
- Baert AL, Knauth M, Sartor K, eds, et al. *MRI of the Lung*. Berlin Heidelberg, Germany: Springer-Verlag; 2009.
- Kauczor HU, Hofmann D, Kreitner KF, et al. Normal and abnormal ventilation: visualization at hyperpolarized He-3 MR Imaging. *Radiology*. 1996;201:564-8.
- Salerno M, Brookeman JR, de Lange EE, Mugler JP 3rd. Hyperpolarized 3He lung imaging at 0.5 Tesla and 1.5 Tesla: a study of susceptibility-induced effects. *Magn Reson Med*. 2005;53:212-6.
- Parraga G, Mathew L, Etemad-Rezai R, McCormack DG, Santyr GE. Hyperpolarized 3He magnetic resonance imaging of ventilation defects in elderly volunteers: initial findings at 3.0 Tesla. *Acad Radiol*. 2008;15:776-85.
- McGloin C, Benattayallah A, Bowtell RW, Fischele S, Moody A, Morgan P, Owers-Bradley JR. *Low Field Lung Imaging Using Hyperpolarized <sup>3</sup>He: Proceedings of the 9th Annual Meeting of the International Society for Magnetic Resonance in Medicine, Glasgow, Scotland, 21-27 April 2001*.
- Bidnosto CP, Choukeife J, Nacher PJ, Tastevin G. In vivo NMR of hyperpolarized 3He in the lung at very low magnetic fields. *J Magn Reson*. 2003;162:122-32.
- Bannier E, Cieslar K, Mosbah K, et al. Hyperpolarized 3He MR for sensitive imaging of ventilation function and treatment efficiency in young cystic fibrosis patients with normal lung function. *Radiology*. 2010;255:225-32.
- Wild JM, Woodhouse N, Paley MN, et al. Comparison between 2D and 3D gradient-echo sequences for MRI of human lung ventilation with hyperpolarized 3He. *Magn Reson Med*. 2004;52:673-8.
- Mata J, Altes T, Christopher J, Mugler JP 3rd, Brookeman J, de Lange E. *Positional Dependence of Small Inferior Ventilation Defects Seen on Hyperpolarized Helium-3 MRI of the Lung: Proceedings of the 9th Annual Meeting of the International Society for Magnetic Resonance in Medicine, Glasgow, Scotland, 21-27 April 2001*.
- Mugler JP 3rd, Salerno M, de Lange EE, Brookeman JR. *Optimized True FISP Hyperpolarized <sup>3</sup>He MRI of the Lung Yields a 3-fold SNR Increase Compared to FLASH: Proceedings of the 10th Annual Meeting of the International Society for Magnetic Resonance in Medicine, Honolulu, Hawaii, 18-24 May 2002*.
- Wild JM, Fischele S, Woodhouse N, et al. Assessment and compensation of susceptibility artifacts in gradient echo MRI of hyperpolarized 3He gas. *Magn Reson Med*. 2003;50:417-22.



24. Woodhouse N, Swift AJ, Wild JM, et al. *Reduction of Ventilated Lung Volumes in Smokers vs Non-smokers as Measured by Single Shot Fast Spin Echo 1H MRI and Hyperpolarized 3He MRI: Proceedings of the 11th Annual Meeting of the International Society for Magnetic Resonance in Medicine, Toronto, Canada, 10-16 July 2003.*
25. Lehmann F, Knitz F, Weiler N, et al. A software tool for analysis and quantification of regional pulmonary ventilation using dynamic hyperpolarized- $(^3\text{He})$ -MRI [German]. *Rofö.* 2004;176:1399-408.
26. Gierada DS, Saam B, Yablonskiy D, Cooper JD, Lefrak SS, Conradi MS. Dynamic echo planar MR imaging of lung ventilation with hyperpolarized  $(^3\text{He})$  in normal subjects and patients with severe emphysema. *NMR Biomed.* 2000;13:176-81.
27. Saam B, Yablonskiy DA, Gierada DS, Conradi MS. Rapid imaging of hyperpolarized gas using EPI. *Magn Reson Med.* 1999;42:507-14.
28. Ruppert K, Brookeman JR, Mugler JP 3rd. *Real-time MR Imaging of Pulmonary Gas-flow Dynamics with Hyperpolarized  $^3\text{He}$ : Proceedings of the 6th Annual Meeting of the International Society for Magnetic Resonance in Medicine, Sidney, Australia, 18-24 April 1998.*
29. Mugler JP 3rd, Brookeman JR, Knight-Scott J, Maier T, de Lange EE, Bogorad PL. *Interleaved Echo-planar Imaging of the Lungs with Hyperpolarized  $^3\text{He}$ : Proceedings of the 6th Annual Meeting of the International Society for Magnetic Resonance in Medicine, Sidney, Australia, 18-24 April 1998.*
30. Tooker AC, Hong KS, McKinstry EL, Costello P, Jolesz FA, Albert MS. Distal airways in humans: dynamic hyperpolarized  $^3\text{He}$  MR imaging—feasibility. *Radiology.* 2003;227:575-9.
31. Holmes JH, Korosec FR, Du J, et al. Imaging of lung ventilation and respiratory dynamics in a single ventilation cycle using hyperpolarized  $\text{He-3}$  MRI. *J Magn Reson Imaging.* 2007; 26:630-6.
32. Mugler JP 3rd, Wang C, Miller GW, et al. Helium-3 diffusion MR imaging of the human lung over multiple time scales. *Acad Radiol.* 2008;15:693-701.
33. Mugler JP 3rd, Brookeman JR, Knight-Scott J, Maier T, de Lange EE, Bogorad PL. *Regional Measurements of the  $^3\text{He}$  Diffusion Coefficient in the Human Lung, Proceedings of the 6th Annual Meeting of the International Society for Magnetic Resonance in Medicine, Sidney, Australia, 18-24 April 1998.*
34. Salerno M, de Lange EE, Altes TA, Truweit JD, Brookeman JR, Mugler JP 3rd. Emphysema: hyperpolarized helium 3 diffusion MR imaging of the lungs compared with spirometric indexes—initial experience. *Radiology.* 2002;222:252-60.
35. Eberle B, Weiler N, Markstaller K, et al. Analysis of intrapulmonary  $\text{O}(2)$  concentration by MR imaging of inhaled hyperpolarized helium-3. *J Appl Physiol.* 1999; 87:2043-52.
36. Deninger AJ, Eberle B, Ebert M, et al. Quantification of regional intrapulmonary oxygen partial pressure evolution during apnea by  $(^3\text{He})$  MRI. *J Magn Reson.* 1999;141:207-16.
37. Fischer MC, Spector ZZ, Ishii M, et al. Single-acquisition sequence for the measurement of oxygen partial pressure by hyperpolarized gas MRI. *Magn Reson Med.* 2004;52:766-73.
38. Deninger AJ, Eberle B, Bermuth J, et al. Assessment of a single-acquisition imaging sequence for oxygen-sensitive  $(^3\text{He})$ -MRI. *Magn Reson Med.* 2002;47:105-14.
39. Hopkins SR, Levin DL, Emami K, et al. Advances in magnetic resonance imaging of lung physiology. *J Appl Physiol.* 2007;102:1244-54.
40. Rizi RR, Baumgardner JE, Ishii M, et al. Determination of regional VA/Q by hyperpolarized  $^3\text{He}$  MRI. *Magn Reson Med.* 2004;52:65-72.
41. Wild JM, Fischele S, Woodhouse N, Paley MN, Kasuboski L, van Beek EJ. 3D volume-localized pO<sub>2</sub> measurement in the human lung with  $^3\text{He}$  MRI. *Magn Reson Med.* 2005;53:1055-64.

## HYPERPOLARIZED $^3\text{He}$ MRI OF COPD POST TEST

Expires: July 15, 2013 Approved for 1.5 ARRT Category A Credits.

1. **COPD is an umbrella term that includes which of the following lung disorders?**
  - a. Interstitial lung disease
  - b. Chronic bronchitis and emphysema
  - c. Tuberculosis and pulmonary embolism
  - d. Radiation-induced pulmonary injuries
2. **COPD is primarily caused from**
  - a. asbestos exposure.
  - b. genetic abnormalities.
  - c. autoimmunity.
  - d. tobacco use.
3. **Which of the following is NOT a morphologic change of the lungs and airways of patients with COPD?**
  - a. Abnormal proliferation of lung tissue
  - b. Enlarged distal airspaces
  - c. Loss of lung tissue
  - d. Thickening of the lung arteries
4. **An advantage of MRI over other imaging modalities is that it**
  - a. requires longer image acquisition times.
  - b. does not require the use of a contrast agent.
  - c. requires patients to be awake.
  - d. does not require the use of ionizing radiation.
5. **Which gases can be used for lung MR imaging?**
  - a. Helium and xenon
  - b. Hydrogen and nitrogen
  - c. Fluorine and radon
  - d. Chlorine and argon
6. **The process used to produce Hyperpolarize helium which involves irradiating the gas with a high powered laser light is known as**
  - a. sublimation.
  - b. optical pumping.
  - c. chromatography.
  - d. spectography.

7. MR imaging of the lung is problematic because of
  - a. high temporal resolution.
  - b. high spatial resolution.
  - c. low air concentration.
  - d. low signal strength.
8. Hyperpolarized helium has significantly improved lung MR imaging because, after its inhalation, the strength of the signal from the lungs
  - a. increases.
  - b. diminishes.
  - c. vibrates.
  - d. collides.
9. Which of the following is NOT important for radio-frequency coils used in hyperpolarized  $^3\text{He}$  MRI?
  - a. They need to cover the field of view of lungs and airways.
  - b. They must be tuned to the Larmor frequency of the gas.
  - c. The excitation angle produced by the transmit coil must be uniform throughout the lungs.
  - d. They must have always the same shape.
10. Hyperpolarized  $^3\text{He}$  MRI is most commonly performed with \_\_\_\_\_ sequences.
  - a. interleaved-spiral
  - b. interleaved echo planar
  - c. low-flip angle fast low-angle shot (FLASH)
  - d. multi-spin echo
11. Hyperpolarized  $^3\text{He}$  MRI includes \_\_\_\_\_ different techniques, each of which provide different information about lung function.
  - a. five
  - b. four
  - c. three
  - d. two
12. Which of the following statements is correct?
  - a. Static ventilation  $^3\text{He}$  MRI detects lung vasculature abnormalities during inspiration.
  - b. Static ventilation  $^3\text{He}$  MRI detects lung ventilation abnormalities during expiration.
  - c. Static ventilation  $^3\text{He}$  MRI detects lung vasculature abnormalities during breath hold.
  - d. Static ventilation  $^3\text{He}$  MRI detects lung ventilation abnormalities during breath hold.
13. In one study of static ventilation hyperpolarized  $^3\text{He}$  MRI, the signal-to-noise ratio achieved for the lungs with 3D sequences was \_\_\_\_\_ times greater than with 2D sequences.
  - a. 2.3
  - b. 1.4
  - c. 1.1
  - d. 0.7
14. In static ventilation hyperpolarized  $^3\text{He}$  MRI, FLASH images of COPD lungs are characterized by marked signal intensity inhomogeneity, with \_\_\_\_\_ areas indicating ventilation defects, and \_\_\_\_\_ areas indicating normal ventilation.
  - a. hypointense; hyperintense
  - b. hyperintense; hypointense
  - c. hyperintense; hyperintense
  - d. hypointense; hypointense
15. Which of the following IS a limitation of static ventilation hyperpolarized  $^3\text{He}$  MRI?
  - a. It uses only FLASH sequences.
  - b. Only 3D acquisitions are possible.
  - c. Volumetric measurements may be difficult.
  - d. Flip angles are too large.
16. Dynamic ventilation  $^3\text{He}$  MRI detects ventilation defects during
  - a. breath hold.
  - b. deglutition.
  - c. breathing.
  - d. rest.
17. Dynamic ventilation images of patients with COPD are characterized by
  - a. nonuniform distribution of the gas throughout the lungs.
  - b. homogeneous distribution of the gas throughout the lungs.
  - c. large, round, focal defects visualized as hyperintense areas.
  - d. a low signal-to-noise ratio.
18. Which of the following sequences is NOT used in dynamic ventilation hyperpolarized  $^3\text{He}$  MRI?
  - a. Interleaved spiral
  - b. Inversion recovery
  - c. Ultra-fast echo-planar (EPI)
  - d. Gradient echo
19. When using an EPI sequence, potential problems in dynamic ventilation hyperpolarized  $^3\text{He}$  MRI include
  - a. side effects from inhaled helium and absent image contrast.
  - b. damage to the coil and excessive  $^3\text{He}$  depolarization.
  - c. long acquisition times and low temporal resolution.
  - d. diffusion-induced signal loss and artifacts.
20. In dynamic ventilation  $^3\text{He}$  MRI increasing the flip-angle value will
  - a. allow more airways to be visualized.
  - b. allow more lung periphery to be visualized.
  - c. reduce the amount of hyperpolarized gas magnetization that is destroyed.
  - d. allow the acquisitions to be obtained during normal breathing.

21. Diffusion hyperpolarized  $^3\text{He}$  MRI allows to assess the lungs' microstructure through measurements of \_\_\_\_\_, using pulsed-gradient spin-echo sequences during breath hold.
- the apparent diffusion coefficient of helium
  - lung ventilation
  - tissue magnetic susceptibility
  - spatial resolution
22. Compared to healthy lungs, hyperpolarized images of COPD lungs show \_\_\_\_\_ ADC values corresponding to \_\_\_\_\_ areas.
- lower; dark
  - higher; bright
  - similar; bright
  - no; dark
23. Which of the following is a potential source of diagnostic errors in diffusion hyperpolarized  $^3\text{He}$  MRI?
- Long diffusion times
  - High signal-to-noise ratio
  - High spatial resolution
  - High temporal resolution
24. Oxygen-sensitive hyperpolarized  $^3\text{He}$  MRI measures \_\_\_\_\_ with \_\_\_\_\_ during breath hold.
- lung microstructure; gradient-echo sequences
  - lung microstructure; echo-planar sequences
  - regional lung function; gradient-echo sequences
  - regional lung function; echo-planar sequences
25. In oxygen-sensitive hyperpolarized  $^3\text{He}$  MRI, which of the following may result in oxygen pressure measurement errors?
- Long image delay times
  - Paramagnetic effects
  - Use of 3D sequences
  - Ventilation defects





Enterprises for Continuing Education, Inc.  
 PO Box 300  
 Brighton, MI 48116-0300  
 Phone: 810-229-3354 Fax: 810-229-3235  
 E-mail: info@cewebsource.com  
 Website: www.cewebsource.com

**CEwebsource.com ANSWER KEY**  
**HYPERPOLARIZED <sup>3</sup>He MRI OF COPD**  
**EXPIRES JULY 15, 2013**

**CEwebsource.com ANSWER SHEET**

Approved by the AHRA for 1.5 Category A CE Credits  
*Please Note: Approved for ARRT and NMTCB Direct Credit*

- Circle the letter corresponding to the correct answer for each question.
- Mail or fax this completed answer sheet along with payment to the address or fax number on the top of this page. If faxing, credit card information must be included.
- You must receive a score of 75% or better to receive credit in any section. Allow up to 4 weeks to process. A Record of Continuing Education will be sent to you.
- Include payment. Answer keys must be accompanied by a \$14 processing fee.
- In a hurry? RUSH SERVICE is available for an additional \$10 for CREDIT CARD ORDERS. Fax this answer key along with your credit card information to (810) 229-3235 for a 48-hour (M-F) turn-around! Whether faxing one answer key or several, only one \$10 charge is added to the total of your order when faxing multiple sheets at once!

**YES**, in addition to the standard processing fee of \$14, please charge my credit card account **\$10 EXTRA for RUSH SERVICE**. FAX my expedited record of Continuing Education to me at: (\_\_\_\_\_) \_\_\_\_\_-\_\_\_\_\_.  
 (If a fax number is not provided, a copy will be sent to the address indicated below within 48 hours)

Method of Payment: (checks payable to **ECEI**)

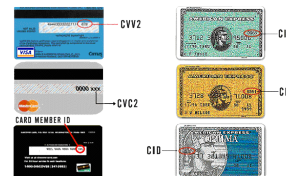
Check  Money Order  Visa  MasterCard  Discover  AmEx

Account Number

V-Code \_\_\_\_\_

Expires \_\_\_\_ / \_\_\_\_



**Identification Section (Please print legibly in blue or black ink):**

Name \_\_\_\_\_ Email \_\_\_\_\_

Address \_\_\_\_\_ Birth Month \_\_\_\_\_

City \_\_\_\_\_ State \_\_\_\_\_ Zip \_\_\_\_\_ Daytime Phone: ( \_\_\_\_\_ ) \_\_\_\_\_ - \_\_\_\_\_

\_\_\_\_\_  
 Previous Name/Zip if changed since your last submission

Please check ONE:  
 MAIL my Record of Continuing Education  
 E-MAIL my Record of Continuing Education

Article Title: **Hyperpolarized <sup>3</sup>He MRI of COPD**

Office Use: MR72/1.5

1. a b c d	6. a b c d	11. a b c d	16. a b c d	21. a b c d
2. a b c d	7. a b c d	12. a b c d	17. a b c d	22. a b c d
3. a b c d	8. a b c d	13. a b c d	18. a b c d	23. a b c d
4. a b c d	9. a b c d	14. a b c d	19. a b c d	24. a b c d
5. a b c d	10. a b c d	15. a b c d	20. a b c d	25. a b c d